IEEE Photonics Journal
An IEEE Photonics Society Publication

Open Access

A Transmission Model of Analog Signals in Photonic Links

Volume 6, Number 6, December 2014

Zhiyu Chen
Lianshan Yan
Wei Pan
Bin Luo
Xihua Zou
Hengyun Jiang

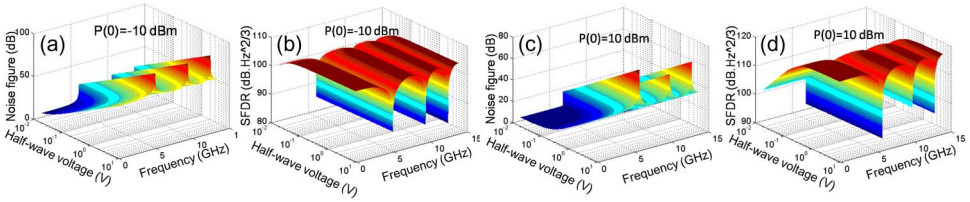

DOI: 10.1109/JPHOT.2014.2366162

IEEE photonics SOCIETY

IEEE

A Transmission Model of Analog Signals in Photonic Links

Zhiyu Chen, Lianshan Yan, Wei Pan, Bin Luo, Xihua Zou, and Hengyun Jiang

Center for Information Photonics and Communications, School of Information Science and Technology, Southwest Jiaotong University, Chengdu 610031, China

DOI: 10.1109/JPHOT.2014.2366162

Manuscript received September 12, 2014; revised October 15, 2014; accepted October 21, 2014. Date of publication November 3, 2014; date of current version November 18, 2014. This work was supported in part by the National Basic Research Program of China under Grant 2012CB315704; by the Natural Science Foundation of China under Grant 61275068, Grant 61335005, and Grant 61325023; and by the Key Grant Project of the Chinese Ministry of Education under Grant 313049. Corresponding author: L. Yan (e-mail: lsyan@home.swjtu.edu.cn).

Abstract: We investigate the transmission of analog photonic signals based on coupled-mode theory and small-signal analysis and provide general expressions for signal evolution along standard single-mode-fiber links. Such model consists of a set of terms that correspond to polarization effects, chromatic dispersion (CD), and fiber nonlinearity. Based on the proposed complete model, we further investigate two typical cases, including the interaction between polarization effects and CD, as well as CD and Kerr effects. In addition, the limitations of the noise figure and spur-free dynamic range are investigated in dispersive nonlinear links.

Index Terms: Analog photonic link, chromatic dispersion, nonlinearity, polarization-mode-dispersion.

1. Introduction

Transmitting analog signals over photonic links is considered to be a promising technique due to the low insertion loss, broad bandwidth and immunity to electromagnetic interference [1], [2]. However, polarization effects, chromatic dispersion (CD) and fiber nonlinearity are three main obstacles for analog photonic signals. The first two impairments contribute to the periodical power fading (PF) [3]–[5], while the last one induces nonlinear distortions [6]–[9], such as self-phase modulation (SPM) [7], [8], cross-phase modulation (XPM) [9], etc. All of them affect the characteristics of frequency response, and limit the performance of analog photonic links (APLs). Therefore, in order to well understand and accurately analyze the signal evolution in APL, it is necessary to develop a mathematical tool for describing the frequency response along the fiber by taking into account the polarization effects, CD and fiber nonlinearities.

In the past two decades, dispersion, fiber nonlinearity and polarization effects have been studied separately for the analog signal transmission in single-mode fiber (SMF). Among them, polarization effects are most difficult to analyze and investigate because the birefringence varies randomly, which induces the polarization mode dispersion (PMD). This random variation in the fiber changes on a time scale of milliseconds to days, so that only the statistical theory can be used to characterize the polarization behavior [10]–[12]. By contrast, the dispersion and Kerr effect are relatively easy to model. The fiber response of the dispersive optical communication

systems based on small signal analysis has been studied in detail [13], [14], and the phase rotation induced by fiber nonlinearity has also been reported by earlier publications [15]. Furthermore, as the transmission distance increases, the interactions between two of them (i.e., nonlinearity and CD, PMD, and CD and nonlinearity and PMD) are investigated in theory and experiment [16]–[25]. For example, when light travels in an optical fiber for thousands of kilometers, the effect of the nonlinearity could no longer be ignored. It can induce the nonlinear polarization rotation or polarization instability in birefringence system [16]–[20] and can be used to counteract CD-induced PF in the dispersive link as well [8], [21], [22]. Especially for [22], it gives a simplified theoretical express to explain such phenomenology. On the other hand, the distortion due to the interaction between CD and PMD is also investigated in many publications [23]–[25]. Previous investigations can be described by the couple nonlinear Schrödinger equation (CNLSE) and Manakov-PMD equations, which are considered as two important mathematical tools for analyzing signal transmission in single-mode fiber (SMF). However, these studies are based on the assumption of ignoring either fiber nonlinearity or birefringence.

In this paper, we establish a propagation model and provide general expressions for the analog signal in photonic links based on the coupled-mode theory and small-signal analysis. Such expressions can be used to describe the frequency response when the signal suffers from polarization effects, CD and fiber nonlinearity simultaneously. In addition, two typical cases are investigated in detail based on the proposed transmission model, i.e., the interaction between polarization effect and CD, and the interaction between CD and fiber nonlinearity. For the first case, the frequency response of the transmitted signal could be expressed by a simple recursion formula. Results indicate that the contribution of PMD is negligible in the standard SMF for the 20-GHz when the transmission distance is 100-km. For the second case, we obtain an analytical solution of the frequency response in the quasi-linear domain. The calculated results show that the CD-induced PF could be mitigated by increasing the input optical power. All analytical calculation results agree well with the previous publications and split-step method. Compared to the conventional split-step approach, the key advantage of our model is the less computation requirements. It is because that the stages of Fourier and inverse Fourier transform are reduced in calculations. Furthermore, the noise figure (NF) and spur-free dynamic range (SFDR) limitations are given for the dispersive nonlinear transmission link, which largely depend on the CD and fiber nonlinearity.

2. Theoretical Model

2.1. Interaction of CD, PMD, and Kerr Effect

SMF used in telecommunications is designed to support only a single mode which, however, exists in two mutually orthogonal polarizations. Due to the imperfect isotropy and asymmetry of the fiber, the two polarization components of the mode travel with different phase and group velocities. When taking into account the CD, PMD, and fiber nonlinearity, a light propagating in SMF obeys the CNLSE [15]

$$\begin{cases} \frac{\partial A_x}{\partial z} + \beta_{1x}\frac{\partial A_x}{\partial t} + \frac{j\beta_{2x}}{2}\frac{\partial^2 A_x}{\partial t^2} + \frac{\alpha}{2}A_x = j\gamma\left(|A_x|^2 + \frac{2}{3}|A_y|^2\right)A_x + \frac{j\gamma}{3}A_x^* A_y^2 \exp(-2j\Delta\beta z) \\ \frac{\partial A_y}{\partial z} + \beta_{1y}\frac{\partial A_y}{\partial t} + \frac{j\beta_{2y}}{2}\frac{\partial^2 A_y}{\partial t^2} + \frac{\alpha}{2}A_y = j\gamma\left(|A_y|^2 + \frac{2}{3}|A_x|^2\right)A_y + \frac{j\gamma}{3}A_y^* A_x^2 \exp(2j\Delta\beta z) \end{cases} \quad (1)$$

where, A_x and A_y are the slowly varying envelope amplitudes for x- and y-polarization. $\beta_{1x,1y}$ and $\beta_{2x,2y}$ are the first and second order differentiations of the propagation constant β. z, α and $\Delta\beta$ (i.e., defined as $|\beta_x - \beta_y|$) are the longitudinal coordinate of the fiber, power attenuation coefficient and birefringence parameter, respectively. γ is the nonlinearity coefficient corresponding to the SPM effect, which is given by $2\pi n_2/(\lambda A_{eff})$ with n_2 as the nonlinear index coefficient and A_{eff} as the effective core area.

In order to simplify (1), we take the transformations as follows:

$$Z = z, \quad T = t - \bar{\beta}_1 z, \quad \bar{\beta}_1 = (\beta_{1x} + \beta_{1y})/2, \quad \beta_{2x} = \beta_{2y} = \beta_2. \tag{2}$$

Subsequently, (1) becomes

$$\begin{cases} \frac{\partial A_x}{\partial Z} + b\frac{\partial A_x}{\partial T} + \frac{j\beta_2}{2}\frac{\partial^2 A_x}{\partial T^2} + \frac{\alpha}{2}A_x = j\gamma\left(|A_x|^2 + \frac{2}{3}|A_y|^2\right)A_x + \frac{j\gamma}{3}A_x^* A_y^2 \exp(-2j\Delta\beta z) \\ \frac{\partial A_y}{\partial Z} - b\frac{\partial A_y}{\partial T} + \frac{j\beta_2}{2}\frac{\partial^2 A_y}{\partial T^2} + \frac{\alpha}{2}A_y = j\gamma\left(|A_y|^2 + \frac{2}{3}|A_x|^2\right)A_y + \frac{j\gamma}{3}A_y^* A_x^2 \exp(2j\Delta\beta z) \end{cases} \tag{3}$$

where b is the specific group delay per unit length, which is represented by $b = \beta_{1x} - \bar{\beta}_1 = (\beta_{1x} - \beta_{1y})/2$. According to [26] and [27], typical SMFs have values $\Delta n \approx 5 \times 10^{-9} \sim 8 \times 10^{-4}$, where Δn is difference in the indexes of refraction between two polarizations. Therefore, when β_2 equals to -20.4 ps^2/km at the wavelength of 1550 nm, the value of b varies between 9.34×10^{-3} and 1.44×10^3 ps/km randomly.

In order to investigate the analog signal evolution through the SMF, we assume that the envelope amplitudes of orthogonal polarizations are $A_{x,y}(Z,T) = \sqrt{P_{x,y}(Z,T)}\exp[j\phi_{x,y}(Z,T)]$ [15]. For convenience, $A_{x,y}$, $P_{x,y}$, and $\phi_{x,y}$ are used to represent $A_x(Z,T)$, $A_y(Z,T)$, $P_x(Z,T)$, $P_y(Z,T)$, $\phi_x(Z,T)$ and $\phi_y(Z,T)$ in the following derivation, respectively. Substituting the envelope amplitudes $A_{x,y}(Z,T)$ into (3), we can obtain

$$\begin{aligned} &\frac{\alpha}{2}\sqrt{P_{x,y}} + \frac{1}{2\sqrt{P_{x,y}}}\frac{\partial P_{x,y}}{\partial Z} + j\sqrt{P_{x,y}}\frac{\partial \phi_{x,y}}{\partial Z} \pm b\frac{1}{2\sqrt{P_{x,y}}}\frac{\partial P_{x,y}}{\partial T} \pm jb\sqrt{P_{x,y}}\frac{\partial \phi_{x,y}}{\partial T} + \frac{j\beta_2}{2\sqrt{P_{x,y}}} \\ &\times\left[-\frac{1}{4P_{x,y}}\left(\frac{\partial P_{x,y}}{\partial T}\right)^2 + j\frac{1}{2}\frac{\partial P_{x,y}\partial \phi_{x,y}}{\partial T\cdot\partial T} + \frac{1}{2}\frac{\partial^2 P_{x,y}}{\partial T^2}\right] - \frac{\beta_2}{2}\sqrt{P_{x,y}}\left[\frac{1}{2P_{x,y}}\frac{\partial P_{x,y}\partial \phi_{x,y}}{\partial T\cdot\partial T} + j\left(\frac{\partial \phi_{x,y}}{\partial T}\right)^2\right] \\ &- \frac{\beta_2}{2}\sqrt{P_{x,y}}\frac{\partial^2 \phi_{x,y}}{\partial T^2} = j\gamma\left(P_{x,y} + \frac{2}{3}P_{y,x}\right)\sqrt{P_{x,y}} + \frac{j\gamma}{3}\sqrt{P_{x,y}}P_{y,x}\exp(-2j\Delta\beta Z). \end{aligned} \tag{4}$$

In order to simplify (4), the small signal analysis is applied [13]. We assume that the intensities of the orthogonal modes are small so that they could be split into time dependent (i.e., $p_{x,y}(Z,T)$) and average components (i.e., $P_{x,y}(Z)$). Therefore, the total powers of two polarizations can be written as $P_{x,y}(Z,T) = P_{x,y}(Z) + p_{x,y}(Z,T)$. When the frequency modulation index is small, the products of $p_{x,y}(Z,T)$ and $\phi_{x,y}(Z,T)$ and their higher-order components can be neglected [13]. Therefore, substituting $P_{x,y}(Z,T)$ into (4), the nonlinear coupled equations become

$$\begin{aligned} &\frac{\partial\left[P_{x,y}(Z) + p_{x,y}\right]}{\partial Z} + j2\left[P_{x,y}(Z) + p_{x,y}\right]\frac{\partial \phi_{x,y}}{\partial Z} \pm b\frac{\partial p_{x,y}}{\partial T} \pm j2b\left[P_{x,y}(Z) + p_{x,y}\right]\frac{\partial \phi_{x,y}}{\partial T} + j\frac{1}{2}\beta_2\frac{\partial^2 p_{x,y}}{\partial T^2} \\ &- \beta_2\left[P_{x,y}(Z) + p_{x,y}\right]\frac{\partial^2 \phi_{x,y}}{\partial T^2} + \alpha\left[P_{x,y}(Z) + p_{x,y}\right] = j2\gamma\left\{\left[P_{x,y}(Z) + p_{x,y}\right] + \frac{2}{3}\left[P_{y,x}(Z) + p_{y,x}\right]\right\} \\ &\cdot\left[P_{x,y}(Z) + p_{x,y}\right] + \frac{j2\gamma}{3}\left[P_{x,y}(Z) + p_{x,y}\right]\cdot\left[P_{y,x}(Z) + p_{y,x}\right]\exp(-2j\Delta\beta Z). \end{aligned} \tag{5}$$

Subsequently, we define the normalized power $p_{N(x,y)}(Z,T)$ as $p_{x,y}(Z,T) = p_{N(x,y)}(Z,T) \times \exp(-\alpha Z)$, and the average components as $P_{x,y}(Z) = P_{x,y}(0)\exp(-\alpha Z)$, where $P_{x,y}(0)$ are the optical average powers of the orthogonal modes at the fiber input. As a result, (5) can be further simplified as

$$\begin{aligned} &-\alpha P_{x,y}(0) - \alpha p_{N(x,y)} + \frac{\partial p_{N(x,y)}}{\partial Z} \pm b\frac{\partial p_{N(x,y)}}{\partial T} + j\frac{1}{2}\beta_2\frac{\partial^2 p_{N(x,y)}}{\partial T^2} \pm j2b\left[P_{x,y}(0) + p_{N(x,y)}\right]\frac{\partial \phi_{x,y}}{\partial T} \\ &- \beta_2\left[P_{x,y}(0) + p_{Nx,y}\right]\frac{\partial^2 \phi_{x,y}}{\partial T^2} + j2\left[P_{x,y}(0) + p_{N(x,y)}\right]\frac{\partial \phi_{x,y}}{\partial Z} + \alpha\left[P_{x,y}(0) + p_{N(x,y)}\right] = Non(Z,T) \end{aligned} \tag{6}$$

where $Non(Z,T)$ is the nonlinearity terms given by

$$Non(Z,T) = j2\gamma\left[P_{x,y}(0) + p_{N(x,y)} + \frac{2}{3}P_{y,x}(0) + \frac{2}{3}p_{N(y,x)}\right] \cdot \left[P_{x,y}(0) + p_{N(x,y)}\right]\exp(-\alpha Z) + \frac{j2\gamma}{3}\left[P_{x,y}(0) + p_{N(x,y)}\right] \cdot \left[P_{y,x}(0) + p_{N(y,x)}\right]\exp(-2j\Delta\beta Z)\exp(-\alpha Z). \quad (7)$$

Separating the real part and imaginary part and making the Fourier transform, (6) becomes

$$\frac{\partial \tilde{p}_{N(x,y)}}{\partial Z} \pm jb\omega\tilde{p}_{N(x,y)} + \beta_2\omega^2 P_{x,y}(0)\tilde{\phi}_{x,y} = \tilde{R}(Non(Z,\omega)) \quad (8a)$$

$$2P_{x,y}(0)\frac{\partial \tilde{\phi}_{x,y}}{\partial Z} \pm 2jb\omega P_{x,y}(0)\tilde{\phi}_{x,y} - \frac{1}{2}\beta_2\omega^2\tilde{p}_{N(x,y)} = \tilde{I}(Non(Z,\omega)) \quad (8b)$$

where $\tilde{p}_{N(x,y)} = \tilde{p}_{N(x,y)}(Z,\omega)$ and $\tilde{\phi}_{x,y} = \tilde{\phi}_{x,y}(Z,\omega)$ are the Fourier transforms of $p_{N(x,y)}(Z,T)$ and $\phi_{x,y}(Z,T)$. $R(x)$ and $I(x)$ indicate the real part and imaginary part of the x. The initial conditions of (8) are

$$\begin{cases} \tilde{p}_{Nx}(0,\omega) = \tilde{p}_{\text{in}}(\omega)\cos^2(\theta), \tilde{p}_{Ny}(0,\omega) = \tilde{p}_{\text{in}}(\omega)\sin^2(\theta) \\ \partial\tilde{p}_{Nx}/\partial Z|_{Z=0} = \tilde{R}(Non(0,\omega)) - jb\omega P_{\text{in}}(0)\cos^2(\theta) - \beta_2\omega^2 P_{\text{in}}(0)\cos^2(\theta)\tilde{\phi}_{\text{in}}(\omega) \\ \partial\tilde{p}_{Ny}/\partial Z|_{Z=0} = \tilde{R}(Non(0,\omega)) + jb\omega P_{\text{in}}(0)\sin^2(\theta) - \beta_2\omega^2 P_{\text{in}}(0)\sin^2(\theta)\tilde{\phi}_{\text{in}}(\omega) \end{cases} \quad (9)$$

where $\tilde{p}_{\text{in}}(\omega)$, $\tilde{\phi}_{\text{in}}(\omega)$, and $P_{\text{in}}(0)$ are the intensity, phase, and average power of the optical signal at the fiber input, respectively. The transmitter chirp is included by the phase modulation (PM) term $\tilde{\phi}_{\text{in}}(\omega)$. θ is the incident angle with respect to the principal axis of the fiber. According to (8a) and (8b), the second terms on the left-hand side lead to the linear PMD effect, which has been discussed in [10] and [11]. It is known that the fast and slow axes are interchanged randomly along the fiber, which depends on the sign of b in (8). The third terms on the left-hand side correspond to the effect of CD. In addition, the terms on the right-hand side of the equations include the nonlinear effects. Therefore, these coupled nonlinear equations govern the power and phase evolution along the SMF by taking into account the PMD, CD, Kerr effect, and fiber loss.

2.2. Interaction Between CD and PMD

If we consider a weak incident light, the nonlinear terms in (8a) and (8b) can be ignored (i.e., $\gamma = 0$). In this case, the equations can be further simplified and only remain the linear terms

$$\frac{\partial \tilde{p}_{N(x,y)}}{\partial Z} \pm jb\omega\tilde{p}_{N(x,y)} + \beta_2\omega^2 P_{x,y}(0)\tilde{\phi}_{x,y} = 0 \quad (10a)$$

$$2P_{x,y}(0)\frac{\partial \tilde{\phi}_{x,y}}{\partial Z} \pm 2jb\omega P_{x,y}(0)\tilde{\phi}_{x,y} - \frac{1}{2}\beta_2\omega^2\tilde{p}_{N(x,y)} = 0. \quad (10b)$$

Here, we only focus on the intensity modulation (IM) solution since the information is recovered from the optical amplitude in IM-direct detection (IM-DD) systems. Thus, differentiating (10a) and eliminating $\tilde{\phi}_{x,y}$ related terms with the help of (10b), the linear equations for analog signal evolution are obtained as follows when we ignore the fiber loss:

$$\frac{\partial^2 \tilde{p}_{N(x,y)}(Z,\omega)}{\partial Z^2} \pm 2jb\omega\frac{\partial \tilde{p}_{N(x,y)}(Z,\omega)}{\partial Z} + \left[\beta_2^2\omega^4/4 - b^2\omega^2\right]\tilde{p}_{N(,y)x}(Z,\omega) = 0. \quad (11)$$

To solve the above equations, we proceed in two successive steps. The detailed derivation process is given in appendix *A*. Here, we simply present the result. First, the transmission distance Z is subdivided into smaller subintervals ΔZ. Using the initial conditions, the solution of (11) may be written as

$$\vec{\tilde{p}}_N(Z,\omega) = R\Big\{\exp\big[j\beta_2\omega^2\Delta Z/2\big]\vec{M}(\omega)\vec{\tilde{p}}_N(Z-\Delta Z,\omega)\Big\} - \vec{\tilde{\phi}}(Z-\Delta Z,\omega)2I\Big\{\exp\big[j\beta_2\omega^2\Delta Z/2\big]\vec{M}(\omega)\vec{\tilde{p}}_N(Z-\Delta Z,\omega)\Big\} \quad (12)$$

where the vectors $\vec{\tilde{p}}_N(Z,\omega)$, $\vec{\tilde{\phi}}(Z,\omega)$, and $\vec{M}(\omega)$ are $[\tilde{p}_{Nx}(Z,\omega);\tilde{p}_{Ny}(Z,\omega)]$, $[\tilde{\phi}_x(Z,\omega);\tilde{\phi}_y(Z,\omega)]$, and $[M_1(\omega),0;0,M_2(\omega)]$, respectively. The value of $\vec{M}(\omega)$ varies rapidly and randomly along the fiber, which depends on the birefringence.

Second, to calculate the term $\vec{M}(\omega)$, we need to further subdivide ΔZ into smaller subintervals δZ due to the fact that the birefringence changes randomly on a length scale of 0.3–100 m. In this case, b is represented by δb_i in each segment. Therefore, $\vec{M}(\omega)$ can be obtained as $\vec{M}(\omega) = \prod_{i=0}^{N}\vec{m}_i(\omega)$, where $\vec{m}_i(\omega)$ is given by $\vec{m}_i(\omega) = [m_{11},0;0,m_{11}^*]$ and $m_{11} = \exp(-j\omega\delta b_i\cdot\delta Z)$.

As can be seen, the obtained equations are similar to (21)–(26) in [25], which indicates the viability of the proposed model. Therefore, the combined output intensity of the fiber is given by $\tilde{p}_N(Z,\omega) = \tilde{p}_{Nx}(Z,\omega) + \tilde{p}_{Ny}(Z,\omega)$.

For microwave photonic links, it usually uses the conversion function of IM-IM (i.e., C_{IM-IM}) to characterize the modulation response. Therefore, according to the definition in [21], the fiber response of the link for intensity modulation becomes

$$C_{IM-IM} = \frac{\tilde{p}_N(Z,\omega)}{\tilde{p}_{\text{in}}(\omega)}\Big|_{\tilde{\phi}_{\text{in}}(\omega)=0} = \sum_{i=1}^{2} R\big\{\exp\big(j\beta_2\omega^2\Delta Z/2\big)M_i(\omega)\tilde{p}_N(Z-\Delta Z,\omega)\big\}. \quad (13)$$

2.3 Interaction Between CD and Kerr Effect

Compared with chromatic dispersion, PMD plays a nearly negligible role in standard SMF links when the transmission distance is smaller than 100 km [28]. For example, if we assume a PMD value of 0.1 ps/km$^{1/2}$ (in fact, this value is much smaller for state-of-art SMF), the average differential group delay is only 1 ps over 100 km transmission. This value is not large enough to significantly distort the individual channels. Therefore, by ignoring PMD, we have $b = 0$, $\tilde{p}_{Nx} = \tilde{p}_N$, $\tilde{p}_{Ny} = 0$, $\tilde{\phi}_x = \tilde{\phi}$, and $\tilde{\phi}_y = 0$.

Previously, some investigations have examined the joint effect of fiber dispersion and nonlinearity in the transmission of single RF carrier [8], [21], [22]. They show that the nonlinear Kerr effect could significantly change the propagation characteristics. As for the frequency response, deep notches move to higher frequency as the optical power at the input fiber increases. However, when the power is large enough, the actual frequency response is different from the calculated one (i.e., the theoretical model used for less power). To further investigate the signal evolution as completely and accurate as possible, we firstly simulate the transmission using a split-step Fourier method [29] applied to the NLSE including fiber dispersion and nonlinearity. The length, dispersion, and nonlinearity of the fiber are 50 km, 16 ps/(nm • km) and 1.852 w^{-1}/km, respectively. As can be seen from Fig. 1(a)–(c), deep notches appear periodically as the transmitted frequency increases. Furthermore, notches move to higher frequency when the input optical power increases from −10 dBm to 13 dBm. However, as the input power further increases, periodical power fading disappears as shown in Fig. 1(d)–(f), and the fluctuation of the response is in the range of 20 dB when the launching power is 20 dBm. Therefore, two different types of behaviors are obtained from simulations. According to [30], these two cases can be defined as quasi-linear domain and irregular domain.

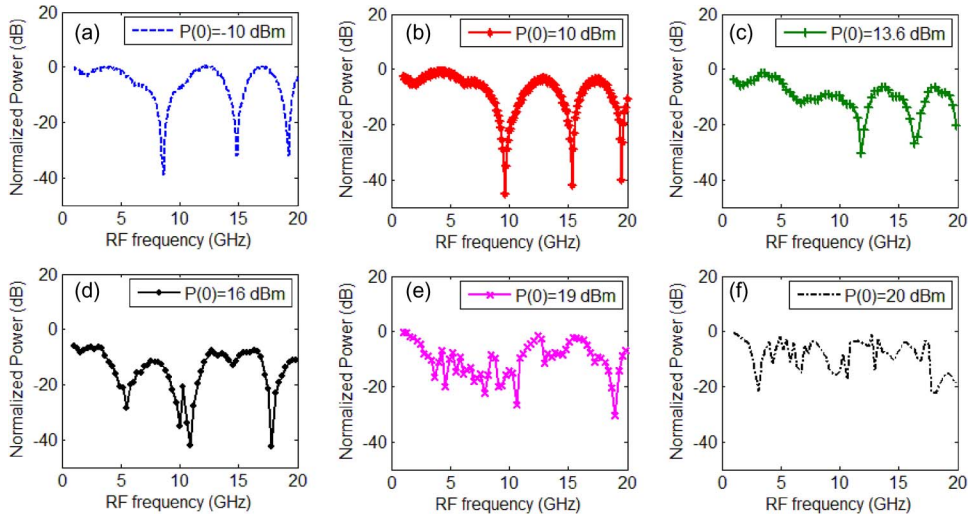

Fig. 1. Fiber response using split-step Fourier method with different input optical powers (P(0)). (a) −10 dBm. (b) 0 dBm. (c) 16 dBm. (d) 19 dBm.

2.3.1. Quasi-Linear Case

First, for a weak incident light, (8a) and (8b) can be rewritten as follows by ignoring the birefringence effect:

$$\frac{\partial \tilde{p}_N}{\partial Z} + \beta_2 \omega^2 P(0)\tilde{\phi} = \tilde{R}(Non(Z,\omega)) \tag{14a}$$

$$2P(0)\frac{\partial \tilde{\phi}}{\partial Z} - \frac{1}{2}\beta_2 \omega^2 \tilde{p}_N = \tilde{I}(Non(Z,\omega)) \tag{14b}$$

where, $Non(Z,T) = j4\gamma P(0) p_N \exp(-\alpha Z)$.

Equations (14a) and (14b) govern the power and phase evolution in the presence of CD and Kerr effect. In [22], for example, a solution for the above equations has been obtained while here we derive a more simple and intuitive expression for IM-DD systems. Similar to the transformation in [22], by differentiating (14a) and further substituting into (14b), we can obtain a second-order differential equation:

$$\frac{\partial^2 \tilde{p}_N}{\partial Z^2} = -\left[\beta_2^2 \omega^4/4 + 2\gamma\beta_2\omega^2 P(0)\exp(-\alpha Z)\right]\tilde{p}_N \tag{15}$$

whose initial conditions are $\tilde{p}_N(0,\omega) = \tilde{p}_{\text{in}}(\omega)$ and $\frac{\partial \tilde{p}_N}{\partial Z}|_{Z=0} = -\beta_2\omega^2 P(0)\tilde{\phi}_{\text{in}}(\omega)$.

Equation (15) has an analytical solution as follows when we neglect the fiber loss

$$\tilde{p}_N = \frac{\tilde{p}_{\text{in}}(\omega)\sqrt{-\beta_2^2\omega^2 - 0.8\gamma P(0)\beta_2} + 2\beta_2\tilde{\phi}_{\text{in}}(\omega)P(0)\omega}{2\sqrt{-\beta_2^2\omega^2 - 0.8\gamma P(0)\beta_2}\exp\left[\frac{1}{2}\omega Z\sqrt{-\beta_2^2\omega^2 - 0.8\gamma P(0)\beta_2}\right]}$$
$$+\frac{\tilde{p}_{\text{in}}(\omega)\sqrt{-\beta_2^2\omega^2 - 0.8\gamma P(0)\beta_2} - 2\beta_2\tilde{\phi}_{\text{in}}(\omega)P(0)\omega}{2\sqrt{-\beta_2^2\omega^2 - 0.8\gamma P(0)\beta_2}}\exp\left[\frac{1}{2}\omega Z\sqrt{-\beta_2^2\omega^2 - 0.8\gamma P(0)\beta_2}\right]. \tag{16}$$

Equation (16) is a general expression to fully characterize the IM signal evolution along the nonlinear dispersive fiber taking into account the interplay between CD and Kerr effect. In this case,

the fiber responses can be given by

$$C_{IM-IM} = R\left\{\exp\left[j\frac{1}{2}\omega Z\sqrt{\beta_2^2\omega^2 + 0.8\gamma P(0)\beta_2}\right]\right\} \tag{17a}$$

$$C_{PM-IM} = \frac{\tilde{p}_N(Z,\omega)}{\tilde{\phi}_{\text{in}}(\omega)}|_{\tilde{p}_{\text{in}}(\omega)=0} = I\left\{\frac{2\beta_2\omega}{\sqrt{\beta_2^2\omega^2 + 0.8\gamma P(0)\beta_2}}\exp\left[\frac{j\omega Z\sqrt{\beta_2^2\omega^2 + 0.8\gamma P(0)\beta_2}}{2}\right]\right\}. \tag{17b}$$

Equations (17a) and (17b) depict the signal evolution well only in quasilinear case, because the proposed theoretical model is based on small signal analysis. Furthermore, in the case of linear propagation $(\gamma = 0)$, (17a) and (17b) can be simplified as $C_{IM-IM}|_{\gamma=0} = \cos\left(\frac{1}{2}\beta_2\omega^2 Z\right)$ and $C_{PM-IM}|_{\gamma=0} = 2\sin\left(\frac{1}{2}\beta_2\omega^2 Z\right)$.

Therefore, the frequency response of IM-DD microwave photonic systems may be directly calculated from these conversion functions as [31]

$$H_F(Z,\omega) = C_{IM-IM}(Z,\omega) + \frac{H_{PM}(\omega)}{2}C_{PM-IM}(Z,\omega) \tag{18}$$

where $H_{PM}(\omega)$ is the optical transmitter response.

2.3.2. Irregular Case

As mentioned above, when the power at the fiber input increases to be larger than 13 dBm for the fiber length of 50 km, the actual measured frequency responses are different from the calculated results by (17a) and (17b). It is because that the product of $p_{x,y}(Z,T)$ and $\phi_{x,y}(Z,T)$ and their high-order components could not be neglected in this case, which leads to more complicated expressions for the signal transmission. The corresponding nonlinear coupled (6) becomes

$$\begin{aligned}&\frac{\partial p_{N(x,y)}}{\partial Z} \pm b\frac{\partial p_{N(x,y)}}{\partial T} + j2\left[P_{x,y}(0) + p_{N(x,y)}\right]\frac{\partial \phi_{x,y}}{\partial Z} \pm j2b\left[P_{x,y}(0) + p_{N(x,y)}\right]\frac{\partial \phi_{x,y}}{\partial T}\\ &+ j\beta_2\left[\frac{\left(\partial p_{N(x,y)}/\partial T\right)^2}{4\left[P_{x,y}(0) + p_{N(x,y)}\right]} + \frac{1}{2}j\frac{\partial p_{N(x,y)}}{\partial T}\frac{\partial \phi_{x,y}}{\partial T} + \frac{1}{2}\frac{\partial^2 p_{N(x,y)}}{\partial T^2}\right] - \frac{\beta_2}{2}\frac{\partial p_{N(x,y)}}{\partial T}\frac{\partial \phi_{x,y}}{\partial T}\\ &- j\beta_2\left[P_{x,y}(0) + p_{N(x,y)}\right]\left(\frac{\partial \phi_{x,y}}{\partial T}\right)^2 - \beta_2\left[P_{x,y}(0) + p_{Nx,y}\right]\frac{\partial^2 \phi_{x,y}}{\partial T^2} = Non(Z,T).\end{aligned} \tag{19}$$

As a result, by separating the real part and imaginary part, and making the Fourier transform, we could get the analog signal transmission function as

$$\frac{\partial \tilde{p}_{N(x,y)}}{\partial Z} + \beta_2\omega^2 P_{x,y}(0)\tilde{\phi} + \frac{\beta_2\omega^2}{\pi}\left(\tilde{p}_{N(x,y)} * \tilde{\phi}_{x,y}\right) = R\left(\tilde{N}on(Z,\omega)\right) \tag{20a}$$

$$\begin{aligned}&2P(0)\frac{\partial \tilde{\phi}_{x,y}}{\partial Z} + \frac{1}{\pi}\tilde{p}_{N(x,y)} * \frac{\partial \tilde{\phi}_{x,y}}{\partial Z} - \frac{1}{2}\beta_2\omega^2\tilde{p}_{N(x,y)} + \frac{\omega^2\beta_2 P_{x,y}(0)}{2\pi}\tilde{\phi}_{x,y} * \tilde{\phi}_{x,y}\\ &+ \frac{\omega^2\beta_2}{4\pi^2}\tilde{\phi}_{x,y} * \tilde{\phi}_{x,y} * \tilde{p}_{N(x,y)} + \frac{\beta_2}{4}F\left[\frac{\left(\partial p_N/\partial T\right)^2}{P(0) + p_N}\right] = \tilde{I}(Non(Z,\omega))\end{aligned} \tag{20b}$$

where function $F[x]$ and operator $*$ indicate the Fourier transform of x and convolution. Unfortunately, (20a) and (20b) do not have the straightforward analytical solutions and only can be solved by using the split-step Fourier method.

2.4 Noise Figure and SFDR Performance

NF and SFDR are two main parameters to evaluate the performance of the APL. Theoretically, when output signal-to-noise ratio (SNR) is at best equal to the input SNR, the minimum NF could achieve 0 dB. However, this value is almost impossible to achieve because relative intensity noise (RIN) or shot noise cannot be totally mitigated. For example, in the APL based on external modulation, the RIN can be neglected compared to the shot noise for the photodetecter currents less than 100 mA. In such link, the dominate source of noise at the PD is the shot noise. Therefore, the expression for the NF is given by $NF = 10\log_{10}\left(2 + \frac{\langle i_{sn}^2\rangle R_{LOAD}}{g_i kT}\right)$ [32], where $\langle i_{sn}^2\rangle$, R_{LOAD}, g_i, and T are mean-square current, load resistance, intrinsic gain, and temperature, respectively. k is Boltzmann's constant, which has a value of 1.38×10^{-23} J/K. As can be seen, the minimum NF for such link is 3 dB (i.e., not 0 dB) as the intrinsic gain goes to infinity. However, previous expression is only suitable for the case of shot-noise-dominated external modulation link. In many practical links, the noise would be altered by the transmission effects such as dispersion and nonlinearity. Therefore, it is important to understand the NF limitation imposed by both the CD and the nonlinearity.

As we all know, for intensity modulated link, the link gain depends on not only the intrinsic gain (i.e., g_i) but also the transmission-induced gain (i.e., PF). In this case, the link gain, g_{link}, can be written in terms of the intrinsic gain and normalized fiber response: $g_{Link} = g_i(\omega)C_{IM-IM}(\omega)$.

Substituting the expressions for shot noise, intrinsic gain of external modulated link with an MZ quadrature-baised modulator [32], and the link gain itself into the expression of NF, we can obtain the NF in quasilinear domain when taking into account the CD and Kerr effect

$$NF = 10\log_{10}\left(2 + \frac{\langle i_{sn}^2\rangle R_{LOAD}}{g_{Link} kT}\right) = 10\log_{10}\left(2 + \frac{2qR_{LOAD}}{C_{IM-IM}(\omega)\cdot\left(\frac{\pi R_s}{2V_\pi}\right)^2 T_{FF} P_I r_d kT}\right) \tag{21}$$

where q, R_s, V_π, T_{FF}, P_I, and r_d are the electron charge, resource resistant, half-wave voltage, attenuation coefficient, input power to the modulator and responsibility of the PD, respectively. As can be seen from (21), the minimum NF is still 3 dB for the dispersive nonlinear link when V_π goes to zero, but this value increases greatly as PF occurs.

It is also useful to examine the impact of the frequency and half-wave voltage on the SFDR performance, which is given by a logarithmic expression $\text{SFDR} = 2 \times [\text{IP}_3 - \text{NF} - (-174)]/3$, where IP_3 is the linearly extrapolated input power in decibels milliwatts as the fundamental and third-order inter-modulation output powers are equal. The constant value of -174 dB refers to the noise power presented in a 1 Hz bandwidth at the standard temperature of 290 K. Here, IP_3 depends on third-order intermodulation suppression (R) and output power (p_N) [33].

3. Results and Comparisons

Based on the above theoretical derivation, we firstly calculate the fiber response as depicted in Fig. 2 when only CD or only PMD presents in APL. The standard SMF parameters are $\beta_2 = -21.6786$ ps2/km (or $D = 17$ ps/km $\cdot$ nm), $\lambda = 1550$ nm, $P(0) = 0$ dB, and $Z = 100$ km. PMD parameters D_{PMD} are set to be 0 ps/$(\text{km})^{1/2}$, 0.1 ps/$(\text{km})^{1/2}$ and 0.5 ps/$(\text{km})^{1/2}$, respectively. The calculated fiber responses of the signal are shown in Fig. 2, where we perform 50 calculations (i.e., considering the statistical behavior of PMD). If D_{PMD} equals to 0 ps/$(\text{km})^{1/2}$, the main distortion to the signal in APL is only CD. Therefore, the periodical deep notches are obtained as the transmitted frequency increases (i.e., Fig. 2(a)), which agrees well with the split-step method (i.e., cross). One the other hand, when $\beta_2 = 0$ and $D_{PMD} = 0.5$ ps/$(\text{km})^{1/2}$, the fiber response with only PMD presents is shown in Fig. 2(b), where the received intensity is proportional to $\cos(2\pi f \cdot DGD)$. The solid line is the maximum theoretical fading curve for 10.7 ps DGD

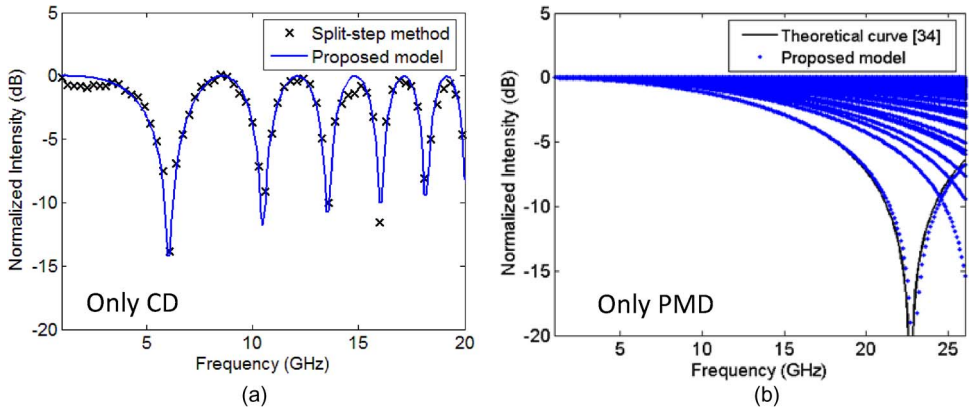

Fig. 2. Calculated fiber responses of the transmitted signal for the length of 100 km when (a) only CD or (b) only PMD presents.

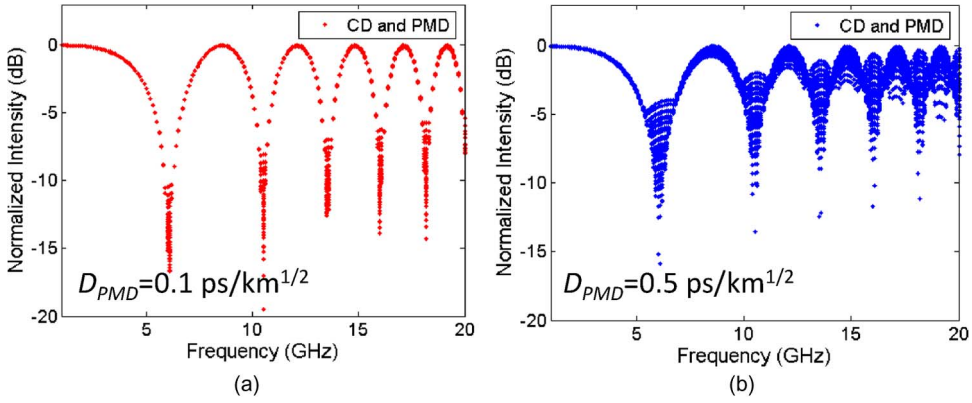

Fig. 3. Calculated fiber responses of the transmitted signal for the length of 100 km when PMD parameter is set to be (a) 0.1 ps/$(\text{km})^{1/2}$ and (b) 0.5 ps/$(\text{km})^{1/2}$.

according to the previous work [34]. As can be seen, the power fading is obtained as well due to the random polarization coupling into the principal-state-of-polarizations (PSPs). Furthermore, the data points of the simulated intensity by using proposed model would fill out the area inside the theoretical fading curve. It is consistent with the [3].

Afterwards, the statistics of the power fading induced by CD and PMD is investigated as shown in Fig. 3. When PMD is set to be 0.1 ps/$(\text{km})^{1/2}$, the pure and periodical notches are still observed (i.e., Fig. 3(a)) because the contribution of PMD is much smaller than that of CD. However, this response characteristic would be changed as shown in Fig. 3(b) when PMD parameter is further increased (i.e., 0.5 ps/$(\text{km})^{1/2}$). It is because the distortion induced by PMD is large enough. In this case, the combination of CD and PMD leads to the aperiodic fading, which needs to be described by using statistics.

Fig. 4 shows the IM-IM conversion for 100-km SMF transmission when the input power are set to be -10 dBm, 10 dBm, and 13 dBm by using proposed scheme and conventional split-step method, respectively. In this case, the nonlinear coefficient of the SMF is set to be 1.852 w^{-1}/km. As shown in Fig. 4(a)–(c), the results calculated by our model agree well with that of the split-step method. The frequency notches of the IM-IM conversion are moved to higher frequencies as the optical power increases. It is because the Kerr effect-induced chirp changes the frequency response of the fiber. As a result, chromatic dispersion in combination with the chirping effect can lead to an improvement of the frequency-length product of the system.

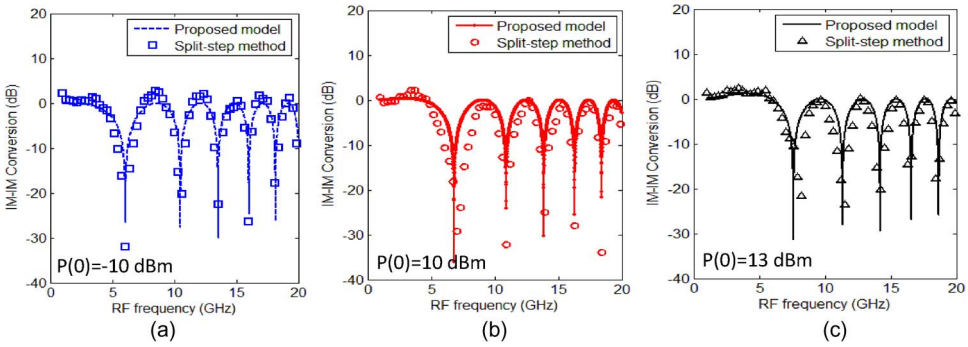

Fig. 4. Calculated IM-IM conversion versus RF frequency for several optical powers at the input of 100-km SMF based on proposed model and conventional split-step method. (a) $P(0) = -10$ dBm. (b) $P(0) = 10$ dBm. (c) $P(0) = 13$ dBm.

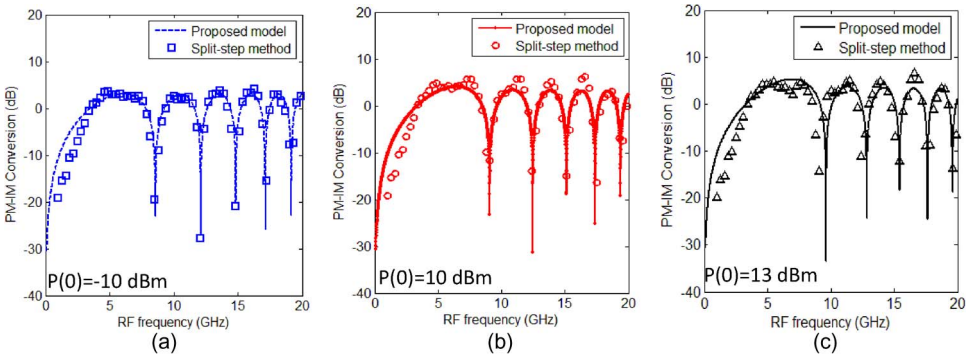

Fig. 5. Calculated PM-IM conversion versus RF frequency for several optical powers at the input of 100-km SMF based on proposed model and conventional split-step method. (a) $P(0) = -10$ dBm. (b) $P(0) = 10$ dBm. (c) $P(0) = 13$ dBm.

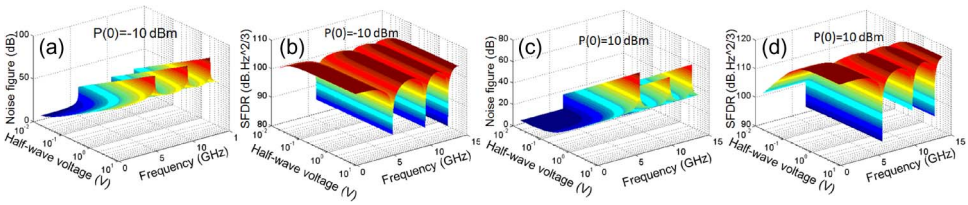

Fig. 6. Calculated NF and SFDR performance in dispersive nonlinear link when changing the half-wave voltage and transmitted frequency for (a), (b) −10 dBm and (c), (d) 10 dBm optical power.

On the other hand, the PM-IM conversion response is also depicted in Fig. 5 for the same parameters as those used for the results shown in Fig. 4. Similar to the IM-IM conversion, as the optical power increases, the frequency response of PM-IM conversion also shifts to the higher frequencies. However, the response is less sensitive to the optical power compared with IM-IM conversion. Compared to the conventional split-step method, our model can provide a faster prediction of the signal transmission trend. In addition, the results shown in Figs. 4 and 5 are consistent with previous works [8], [22] as well, which further indicate that the viability of our proposed model.

Fig. 6 shows the calculated NF and SFDR performance in dispersive nonlinear link when changing the half-wave voltage and transmitted frequency for (a), (b) −10 dBm and (c), (d) 10 dBm. All parameters are the same with [32]. Intuitively, the decreased half-wave voltage

reduces the noise figure, which could improve the link's ability to detect smaller signals. Meanwhile, the SFDR also degrades significantly. Particularly in the region of where noise figure is independent of V_π, the SFDR decreases quadratically with the voltage. However, the characteristics change when the transmitted frequency increases. It is because the CD-induced PF would greatly increase the NF and decrease SFDR as shown in Fig. 6(a)–(d). Furthermore, when the input power is increased, the distortion frequency shifts to higher frequency as depicted previously. Therefore, the fiber nonlinearity can be used to enhance the performance of the APL for a certain transmitted frequency.

4. Discussion and Conclusion

We have established a complete propagation model and provided general expressions for the APL based on coupled-mode theory and small-signal analysis. We found that these expressions consist of a set of terms that correspond physically to polarization effect, chromatic dispersion and fiber nonlinearity. Therefore, they could depict the analog signal evolution in fiber more completely. To illustrate the effectiveness and accuracy of the complete model, we further investigate two simplified cases by ignoring either Kerr or polarization effect. The analytical calculation results for these two typical cases agree well with previous publications and split-step method. In addition, the NF and SFDR for the dispersive nonlinear link have been numerically investigated. Calculated results show that the performance of the link would be degraded significantly due to CD-induced PF.

Although the proposed theory is more complete, we have to note that there are still some limitations: i) the optical power could not be too high because the proposed theoretical derivation is based on small signal analysis, and such model works well in both linear and quasilinear domains; ii) discussions about the interaction between PMD and nonlinearity is not included as it has been investigated in details in [19] and [20].

Appendix A

When signal transmits the distance of ΔZ, (11) for x-polarization can be easily solved as follows by using the initial conditions

$$\tilde{p}_{Nx}(\Delta Z,\omega)=\frac{2j\beta_2\omega\tilde{\phi}_x(0,\omega)\tilde{p}_{Nx}(0,\omega)}{2\beta_2\omega\exp j\Delta Zb\omega}\left[\exp(j\Delta Z\beta_2\omega^2/2)-\exp(-j\Delta Z\beta_2\omega^2/2)\right]+\frac{\beta_2\omega\tilde{p}_{Nx}(0,\omega)}{2\beta_2\omega\exp j\Delta Zb\omega}\left[\exp(j\Delta Z\beta_2\omega^2/2)+\exp(-j\Delta Z\beta_2\omega^2/2)\right] \quad \text{(A1)}$$

By using the equations $\exp(\mathrm{j}x)+[\exp(\mathrm{j}x)]^*=2R\{\exp(\mathrm{j}x)\}$ and $\exp(\mathrm{j}x)-[\exp(\mathrm{j}x)]^*=2\mathrm{j}I\{\exp(\mathrm{j}x)\}$, (A1) can be simplified as

$$\tilde{p}_{Nx}(\Delta Z,\omega)=R\left\{\exp(j\Delta Z\beta_2\omega^2/2)\exp(-j\Delta Zb\omega)\tilde{p}_{Nx}(0,\omega)\right\}-\tilde{\phi}_x(0,\omega)2I\left\{\exp(j\Delta Z\beta_2\omega^2/2)\exp(-j\Delta Zb\omega)\tilde{p}_{Nx}(0,\omega)\right\}. \quad \text{(A2)}$$

To calculate (A2) accurately, subinterval ΔZ needs to be further subdivided into δZ due to the fact that the birefringence changes randomly on a length scale of 0.3–100 m. In this case, b is represented by δb_i in each segment, and the term $\Delta Z\cdot b$ of (A2) becomes $\prod_{i=0}^{N}\delta b_i\delta Z$.

Therefore, the general expression for Z transmission can be expressed by a recursion formula

$$\tilde{p}_{N(x,y)}(Z,\omega)=R\left\{\exp(j\Delta Z\beta_2\omega^2/2)\exp\left[\mp j\omega\left(\prod_{i=0}^{N}\delta b_i\delta Z\right)\right]\tilde{p}_{N(x,y)}(Z-\Delta Z,\omega)\right\}-\tilde{\phi}_{x,y}(Z-\Delta Z,\omega)2I\left\{\exp(j\Delta Z\beta_2\omega^2/2)\exp\left[\mp j\omega\left(\prod_{i=0}^{N}\delta b_i\delta Z\right)\right]\tilde{p}_{N(x,y)}(Z-\Delta Z,\omega)\right\}. \quad \text{(A3)}$$

The vector of spectral power $\vec{\tilde{p}}_N(Z,\omega)$ can be written as

$$\vec{\tilde{p}}_N(Z,\omega) = R\Big\{\exp[j\beta_2\omega^2\Delta Z/2]\vec{M}(\omega)\vec{\tilde{p}}_N(Z-\Delta Z,\omega)\Big\} - \vec{\tilde{\phi}}(Z-\Delta Z,\omega)2I\Big\{\exp(j\Delta Z\beta_2\omega^2/2)\vec{M}(\omega)\vec{\tilde{p}}_N(Z-\Delta Z,\omega)\Big\} \quad \text{(A4)}$$

where $M(\omega) = \prod_{i=0}^{N} m_i(\omega)$, $m_i(\omega) = [m_{11}, 0; 0, m_{11}^*]$, and $m_{11} = \exp(-j\omega\delta b_i \cdot \delta Z)$.

References

[1] J. P. Yao, "Microwave photonics," *J. Lightw. Technol.*, vol. 27, no. 3, pp. 314–355, Feb. 2009.
[2] A. Seeds and K. J. Williams, "Microwave photonics," *J. Lightw. Technol.*, vol. 24, no. 12, pp. 4628–4641, Dec. 2006.
[3] O. H. Adamczyk, A. B. Sahin, Q. Yu, S. Lee, and A. E. Willner, "Statistics of PMD-induced power fading for intensity-modulated double-sideband and single-sideband microwave and millimeter-wave signals," *IEEE Trans. Microw. Theory Tech.*, vol. 49, no. 10, pp. 1962–1967, Oct. 2001.
[4] Z. Y. Chen *et al.*, "Pre-distortion compensation of dispersion in APL based on DSB modulation," *IEEE Photon. Technol. Lett.*, vol. 25, no. 12, pp. 1129–1132, Jun. 2013.
[5] Z. Y. Chen *et al.*, "SFDR enhancement in analog photonic links by simultaneous compensation for dispersion and nonlinearity," *Opt. Exp.*, vol. 21, no. 17, pp. 20 999–21 009, Aug. 2013.
[6] X. Qi, J. Liu, X. Zhang, and L. Xie, "Fiber dispersion and nonlinearity influences on transmissions of AM and FM data modulation signals in radio-over-fiber system," *IEEE J. Quantum Electron.*, vol. 46, no. 8, pp. 1170–1177, Aug. 2010.
[7] C. Desem, "Composite second order distortion due to self-phase modulation in externally modulated optical AM-SCM systems operating at 1550 nm," *Electron. Lett.*, vol. 30, no. 24, pp. 2055–2056, Nov. 1994.
[8] F. Ramos, J. Marti, V. Polo, and J. M. Fuster, "On the use of fiber-induced self-phase modulation to reduce chromatic dispersion effects in microwave/millimeter-wave optical systems," *IEEE Photon. Technol. Lett.*, vol. 10, no. 10, pp. 1473–1475, Oct. 1998.
[9] L. Cheng, S. Aditya, Z. Li, A. Alphones, and M. Ong, "Nonlinear distortion due to XPM in dispersive WDM microwave fiber-optic links with optical SSB modulation," presented at the Int. Topical Meeting Microwave Photonics, Seoul, Korea, Paper TP-31.
[10] C. D. Poole, "Statistical treatment of polarization dispersion in single-mode fiber," *Opt. Lett.*, vol. 13, no. 8, pp. 687–689, Aug. 1988.
[11] G. J. Foschini and C. D. Poole, "Statistical theory of polarization dispersion in single mode fibers," *J. Lightw. Technol.*, vol. 9, no. 11, pp. 1439–1456, Nov. 1991.
[12] D. van den Borne, N. E. Hecker-Denschlag, G. D. Khoe, and H. de Waardt, "PMD-induced transmission penalties in polarization-multiplexed transmission," *J. Lightw. Technol.*, vol. 23, no. 12, pp. 4004–4015, Dec. 2005.
[13] J. Wang and K. Petermann, "Small signal analysis for dispersive optical fiber communication systems," *J. Lightw. Technol.*, vol. 10, no. 1, pp. 96–100, Jan. 1992.
[14] L. H. Cheng, S. Aditya, and A. Nirmalathas, "An exact analytical model for dispersive transmission in microwave fiber-optic links using Mach–Zehnder external modulator," *IEEE Photon. Technol. Lett.*, vol. 17, no. 7, pp. 1525–1527, Jul. 2005.
[15] G. Agrawal, *Nonlinear Fiber Optics*, 2nd ed. San Diego, CA, USA: Academic, 1995.
[16] P. D. Maker and R. W. Terhune, "Study of optical effects due to an induced polarization third order in the electric field strength," *Phys. Rev.*, vol. 137, no. 3A, pp. A801–A818, Feb. 1965.
[17] S. Wabnitz, "Modulational polarization instability of light in a nonlinear birefringent dispersive medium," *Phys. Rev. A, At. Mol. Opt. Phys.*, vol. 38, no. 4, pp. 2018–2021, Aug. 1988.
[18] G. Gregori and S. Wabnitz, "New exact solutions and bifurcations in the spatial distribution of polarization in third-order nonlinear optical interaction," *Phys. Rev. Lett.*, vol. 56, no. 6, pp. 600–603, Feb. 1986.
[19] C. R. Menyuk and B. S. Marks, "Interaction of polarization mode dispersion and nonlinearity in optical fiber transmission systems," *J. Lightw. Technol.*, vol. 24, no. 7, pp. 2806–2826, Jul. 2006.
[20] M. Karlsson and H. Sunnerud, "Effects of nonlinearities on PMD-induced system impairments," *J. Lightw. Technol.*, vol. 24, no. 11, pp. 4127–4137, Nov. 2006.
[21] A. V. T. Cartaxo, B. Wedding, and W. Idler, "Influence of fiber nonlinearity on the phase noise to intensity noise conversion in fiber transmission: Theoretical and experimental analysis," *J. Lightw. Technol.*, vol. 16, no. 7, pp. 1187–1194, Jul. 1998.
[22] F. Ramos and J. Martí, "Frequency transfer function of dispersive and nonlinear single-mode optical fibers in microwave optical systems," *IEEE Photon. Technol. Lett.*, vol. 12, no. 5, pp. 549–551, May 2000.
[23] C. D. Poole and C. R. Giles, "Polarization-dependent pulse compression and broadening due to polarization dispersion in dispersion-shifted fiber," *Opt. Lett.*, vol. 13, no. 2, pp. 155–157, Feb. 1988.
[24] C. D. Poole and T. E. Darcie, "Distortion related to polarization-mode dispersion in analog lightwave systems," *J. Lightw. Technol.*, vol. 11, no. 11, pp. 1749–1759, Nov. 1993.
[25] D. Marcuse, C. R. Menyuk, and P. K. A. Wai, "Application of the Manakov-PMD equation to studies of signal propagation in optical fibers with randomly varying birefringence," *J. Lightw. Technol.*, vol. 15, no. 9, pp. 1735–1746, Sep. 1997.
[26] I. P. Kaminow, "Polarization in optical fibers," *IEEE J. Quantum Electron.*, vol. QE-17, no. 1, pp. 15–22, Jan. 1981.
[27] C. R. Menyuk, "Nonlinear pulse propagation in birefringent optical fiber," *IEEE J. Quantum Electron.*, vol. QE-23, no. 2, pp. 174–176, Feb. 1987.

[28] D. Wang and C. R. Menyuk, "Polarization evolution due to the Kerr nonlinearity and chromatic dispersion," *J. Lightw. Technol.*, vol. 17, no. 12, pp. 2520–2529, Dec. 1999.
[29] A. Hasegawa and F. Tappert, "Transmission of stationary nonlinear optical pulses in dispersive dielectric fibers. I. Anomalous dispersion," *Appl. Phys. Lett.*, vol. 23, no. 142, pp. 142–144, Apr. 1973.
[30] I. Frigyes, Z. Virallyay, O. Schwelb, L. Jakab, and P. Richter, "Investigations in the joint effect of fiber dispersion and nonlinear refraction in microwave optical links," in *Proc. Int. Topical Meet. MWP*, 2003, pp. 299–302.
[31] L. Bjerkan, A. Rgyset, L. Hafskjaer, and D. Myhre, "Measurement of laser parameters for simulation of high-speed fiberoptic systems," *J. Lightw. Technol.*, vol. 14, no. 5, pp. 839–850, May 1996.
[32] C. H. Cox, *Analog Optical Links: Theory and Practice*. Cambridge, U.K.: Cambridge Univ. Press, 2004.
[33] N. G. Kanaglekar, R. E. Mcintosh, and W. E. Bryant, "Analysis of two-tone, third-order distortion in cascaded two-ports," *IEEE Trans. Microw. Theory Tech.*, vol. 36, no. 4, pp. 701–705, Apr. 1988.
[34] H. Schmuck, "Effect of polarization-mode-dispersion in fiber-optic millimeter-wave systems," *Electron. Lett.*, vol. 30, no. 18, pp. 1503–1504, Sep. 1994.